SSRG International Journal of Electrical and Electronics Engineering
ISSN: 2348-8379/ https://doi.org/10.14445/23488379/IJEEE-V12I5P120

Volume 12 Issue 5, 243-252, May 2025

Original Article

Robust Decentralized Load-Frequency-Control of Multi-Area Power Systems with RES and HVDC: A Composite PI$^{\lambda1}$D-PI$^{\lambda2}$DF and Fuzzy-PID Approach

Ngoc-Khoat Nguyen[1*], Diem-Vuong Doan[1]

[1]*Faculty of Control and Automation, Electric Power University, Hanoi, Vietnam.*

[*]*Corresponding Author : khoatnn@epu.edu.vn*

Received: 16 March 2025 Revised: 20 April 2025 Accepted: 02 May 2025 Published: 31 May 2025

Abstract *- The operational stability of modern interconnected power systems globally is increasingly challenged by inherent parametric uncertainties and nonlinearities, leading to significant deviations from nominal system frequency (50Hz or 60Hz). The problem is further complicated by the escalating incorporation of intermittent renewables, including wind and solar power, leading to a notable reduction in system inertia and impaired frequency regulation. To mitigate these adverse effects, this study introduces a novel control strategy: an Improved Grey Wolf Optimization (iGWO)-tuned Fuzzy-PID controller integrated with a PI$^{\lambda1}$D-PI$^{\lambda2}$DF model. This strategy is tailored to achieve frequency stabilization within a multifaceted four-area interconnected electrical network. A key contribution of this work is its explicit modeling of intricate system dynamics, including nonlinear characteristics, HVDC (High-Voltage Direct Current) transmission interconnections, and wind energy generation dynamics. The proposed control strategy's effectiveness and superiority are rigorously validated through comparative simulations under various load change scenarios, contrasting its performance against conventional GWO-tuned PID and standard PID controllers. These comparisons highlight the significant strengths of the iGWO-optimized Fuzzy-PID controller in addressing the complex challenges inherent in contemporary interconnected power systems.*

Keywords *- Hybrid controller, Fuzzy-PID, Fractional PID, LFC, iGWO, HVDC, RESs.*

1. Introduction

National power systems function as critical infrastructure, analogous to the circulatory system within a biological organism. Voltage and frequency constitute essential metrics for the holistic evaluation of power quality. System frequency, a global system variable, exhibits deviations directly attributable to imbalances between power generation and load demand. The inherent stochasticity of electrical load profiles precipitates transient frequency perturbations and deviations from the designated nominal operating frequency (50Hz or 60Hz, as dictated by national standards).

Frequency deviations within an electrical power system can induce faults at generation sources by introducing harmonic distortions. In interconnected power generation facilities, particularly those operating in parallel configurations, maintaining a stable and consistent frequency is essential for synchronous generator operation. Moreover, the operational integrity of numerous electrical devices within a multi-node power network depends on frequency adherence to nominal values. This leads to significant deviations resulting in operational anomalies or complete failure. A substantial reduction in system frequency increases the magnetizing current in inductive loads, such as induction motors and transformers.

The escalating need for electricity has led to the widespread adoption of renewable energy sources within today's power grids. While renewable energy integration offers numerous benefits, it also presents inherent challenges. In interconnected power grids, Renewable Energy Sources (RESs) contribute to increased system nonlinearity. Specifically, wind power generation, characterized by low rotational inertia and an inverter-dependent dynamic response, introduces unique challenges. As the share of wind power in the generation mix increases, system inertia and damping coefficients decrease, heightening the power system's vulnerability to instability. This reduction in inertia and damping exacerbates frequency oscillations and increases the risk of system-wide failures.

Numerous studies have addressed the LFC problem in the case of embedding RESs. In [1], an adaptive Model Predictive Control (MPC) scheme was examined for a power system incorporating wind-based RES. Study [2] implemented the Frequency Domain Analysis (FDA) method on a large-scale power system, considering a diverse RES portfolio encompassing wind energy, Photovoltaic (PV) systems, and Superconducting Magnetic Energy Storage (SMES) units. In [3], a virtual inertia control strategy was explored for controlling the network frequency in an interconnected power system with two interconnected areas featuring wind and solar RES. Numerous prior investigations have explored diverse control mechanisms to augment the frequency stability of power systems. For instance, one study introduced an inner-loop control scheme aimed at bolstering system frequency steadiness [4]. Fuzzy Proportional-Integral-Derivative (PID) regulators, with their parameters fine-tuned by metaheuristics such as the cuckoo search algorithm [4] or the Bacterial Foraging Optimization Algorithm (BFOA) [5], have been central to stabilizing frequency in various grid configurations, including two-area systems featuring renewable energy sources. Hybrid optimization methodologies, like a BFOA-Particle Swarm Optimization (PSO) controller [6], have also been instrumental in calibrating control parameters within intricate hybrid power system architectures.

Beyond conventional PID paradigms, more advanced approaches have emerged. A neural network-based integral sliding mode control strategy was employed for frequency stabilization within power systems experiencing significant wind energy penetration [7]. Furthermore, model predictive control frameworks have been examined for both regulating frequency and supplying synthetic rotational inertia to renewable energy installations [8]. Other notable contributions include the deployment of Hybrid Algorithms (HA) [9] for the parametric optimization of PID controllers in wind-integrated systems and the application of the Butterfly Search Algorithm (BSA) for generalized frequency stabilization efforts [10].

The efficacy of various nature-inspired optimization algorithms in this domain is extensively documented. PSO has been applied to achieve frequency equilibrium in two-area interconnected power systems, taking into account renewable energy source assimilation [11]. The Butterfly Optimization Algorithm (BOA) was investigated for load frequency regulation in an electric power grid encompassing thermal, wind, and solar energy sources [12]. Additionally, the combined particle swarm optimization-grey wolf optimization (PSO-GWO) technique [13] and the Imperialist Competitive Algorithm (ICA) paired with a PID controller [14] have been leveraged for load frequency regulation in photovoltaic-integrated and general power systems, respectively. More recently, the moth-flame algorithm (MBA) has demonstrated potential for the parametric adjustment of PID controllers within systems incorporating SMES units [15] and for fine-tuning PID parameters in complex hybrid power systems characterized by the incorporation of solar, thermal, wind, and diesel energy sources [16].

This investigation delves into a four-area power system, encompassing reheat turbine generators, High-Voltage Direct Current (HVDC) transmission lines, wind power generation, and intrinsic system nonlinearities. The performance of our proposed control approach is meticulously evaluated through a comparative assessment. We benchmark it against systems employing a hybrid grey wolf optimization-tuned Proportional-Integral-Derivative (GWO-PID) controller and standard PID controllers. These efficacy comparisons are presented via simulation outcomes under diverse load perturbation scenarios, all conducted within the MATLAB/Simulink environment.

This paper is organized as follows. Section 2 presents a typical model of a four-area interconnected power system with HVDC links and RESs. Then, Section 3 will investigate a hybrid controller as a newly efficient integration of the $PI^{\lambda 1}D$ - $PI^{\lambda 2}DF$ and Fuzzy-PID controllers together with the *i*GWO algorithm to optimize a number of significant parameters. To demonstrate the control performance and applicability of the proposed control strategy, Section 4 will provide numerous simulations using MATLAB software in comparison with other existing load-frequency controllers. Finally, conclusions and discussions will be deduced in the last section of this paper.

2. Mathematical Model of Interconnected Power System

A large-scale electric power grid, typically called an interconnected power system, typically consists of many subsystems, which can be defined as control areas. Each control area, simply an area, is considered a conventional generation combination that includes a governor, turbine, and generator with embedded loads. The system under this study is a 4-control-area electric power grid, with each area being a reheat turbine. The system considers HVDC and the participation of RESs. The research focused on an interconnected thermal power system consisting of four zones with capacities of 2,000 MW (Area 1), 4,000 MW (Area 2), 8,000 MW (Area 3), and 10,000 MW (Area 4). Additionally, Generation Rate Constraint (GRC) limits the rate of power change due to the physical limitation of the turbine, which is also a factor that causes nonlinearity in the power system. It greatly affects the power system because of its nonlinear nature.

The escalating global energy demand has precipitated a heightened reliance on renewable energy sources, with wind energy emerging as a pivotal contributor. The present investigation employs a 5-MW offshore wind turbine model. This model was developed by the National Renewable Energy Laboratory (NREL) with financial support from the

U.S. Department of Energy under its Wind Energy Technologies Program. This specific model functions as a paramount benchmark for global research endeavors, standardization initiatives, and the comprehensive evaluation of advancements in wind energy technology benefits. While its nominal 5 MW capacity presently surpasses the typical scales in the industry, the significant allocation of capital expenditure towards essential support infrastructure in offshore wind farms inherently necessitates a minimum turbine capacity of 5 MW to guarantee economic viability. The operational efficacy of wind power generation is fundamentally contingent upon the proficiency with which wind kinetic energy is transformed into usable electrical energy.

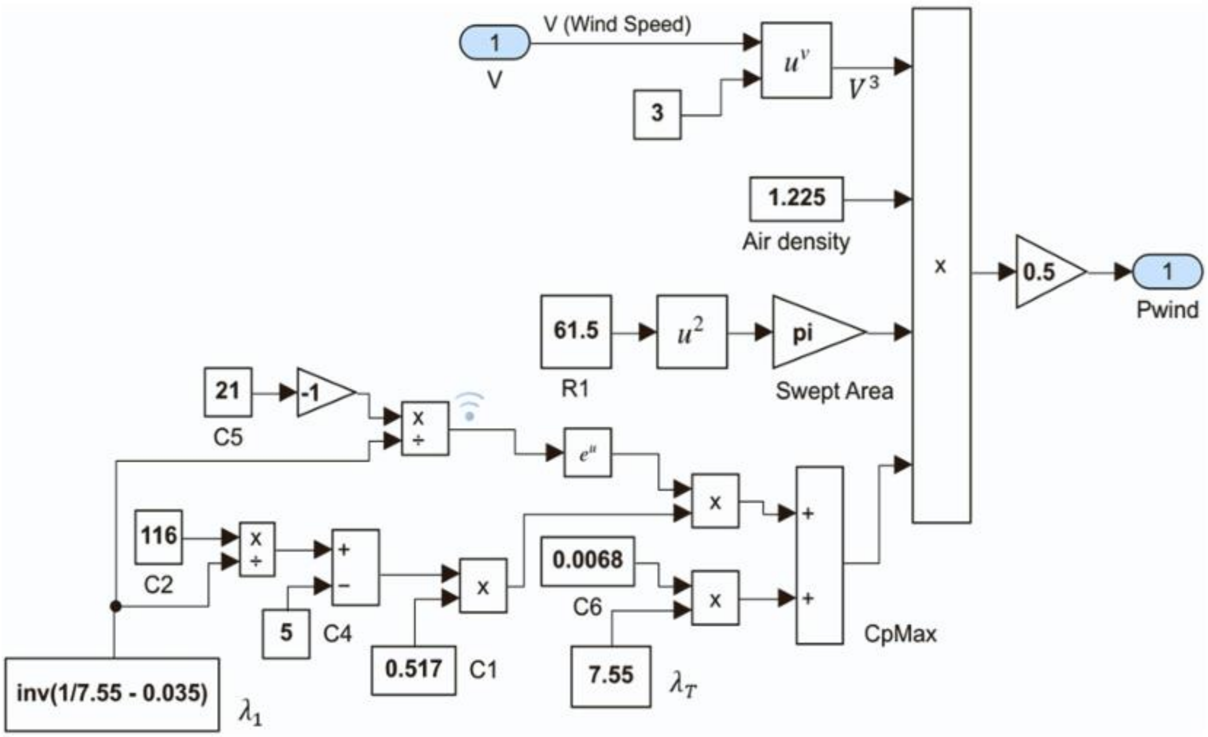

Fig. 1 Model of NREL 5-MW wind turbine built on MATLAB/Simulink [20]

This intricate conversion sequence begins with the aerodynamic capture of wind's energy by the turbine rotor blades, which directly leads to the transmutation of kinetic energy into mechanical rotational energy. Subsequently, an electromechanical generator critically facilitates the transduction of this mechanical rotational energy into electrical energy.

A meticulously crafted simulation model of the NREL 5-Megawatt (MW) wind turbine has been developed and robustly implemented within the MATLAB/Simulink environment, visually presented in Figure 1. This simulation accurately encapsulates the wind turbine system's inherent dynamic behavior and complex energy conversion processes, thereby facilitating exhaustive analysis and performance appraisal. Complementing this, a four-area interconnected power system model incorporating HVDC links has also been constructed in MATLAB/Simulink and seamlessly integrated with these NREL turbine representations, as depicted in Figure 2. This holistic system model will be strategically employed for the rigorous validation of the load-frequency controllers, which will be detailed in the subsequent section.

3. Design of Proposed Hybrid Load–Frequency Controller

Within this section, a novel hybrid load-frequency controller is introduced. The intricate architecture of this proposed control structure is precisely elucidated in Figure 3. This design meticulously combines a Proportional-Fractional Integrator controller with a PID regulator and finally with a filter (PI-D-filter) controller. Subsequently, this integrated combination is further fused with a fuzzy-PID model, thereby constructing the complete hybrid load-frequency controller. Notably, this controller's initial two constituent parts are specifically defined as fractional-order PID controllers, which are recognized for delivering superior control performance owing to their inherent capacity to dynamically adjust their internal structure to precisely adapt to the unique characteristics of a given control system.

As shown in Figure 3, a set of coefficients $K_1, K_2, K_3, \lambda_1, K_P, K_I, K_D, \lambda_1, N$ is optimized using an efficient optimization method, an improved grey wolf optimizer (*i*GWO) method according to a suitable objective function. The GWO algorithm draws its inspiration from the intricate social hierarchy and cooperative hunting tactics observed in wild grey wolves. At its core, GWO designates three leader wolves α, β, and δ —as the prime solutions, guiding the remaining pack members, termed ω wolves, toward optimal regions within the search space to locate the global solution. The fundamental hunting sequence involves three distinct phases: encircling the target, the pursuit itself, and finally, the attack.

However, a key limitation of the GWO lies in how α, β, and δ direct the ω wolves. This approach can lead to premature convergence on local optima, consequently diminishing population diversity and hindering the algorithm's ability to explore the search space effectively. To address these identified shortcomings, this section introduces an improved GWO (*i*GWO).

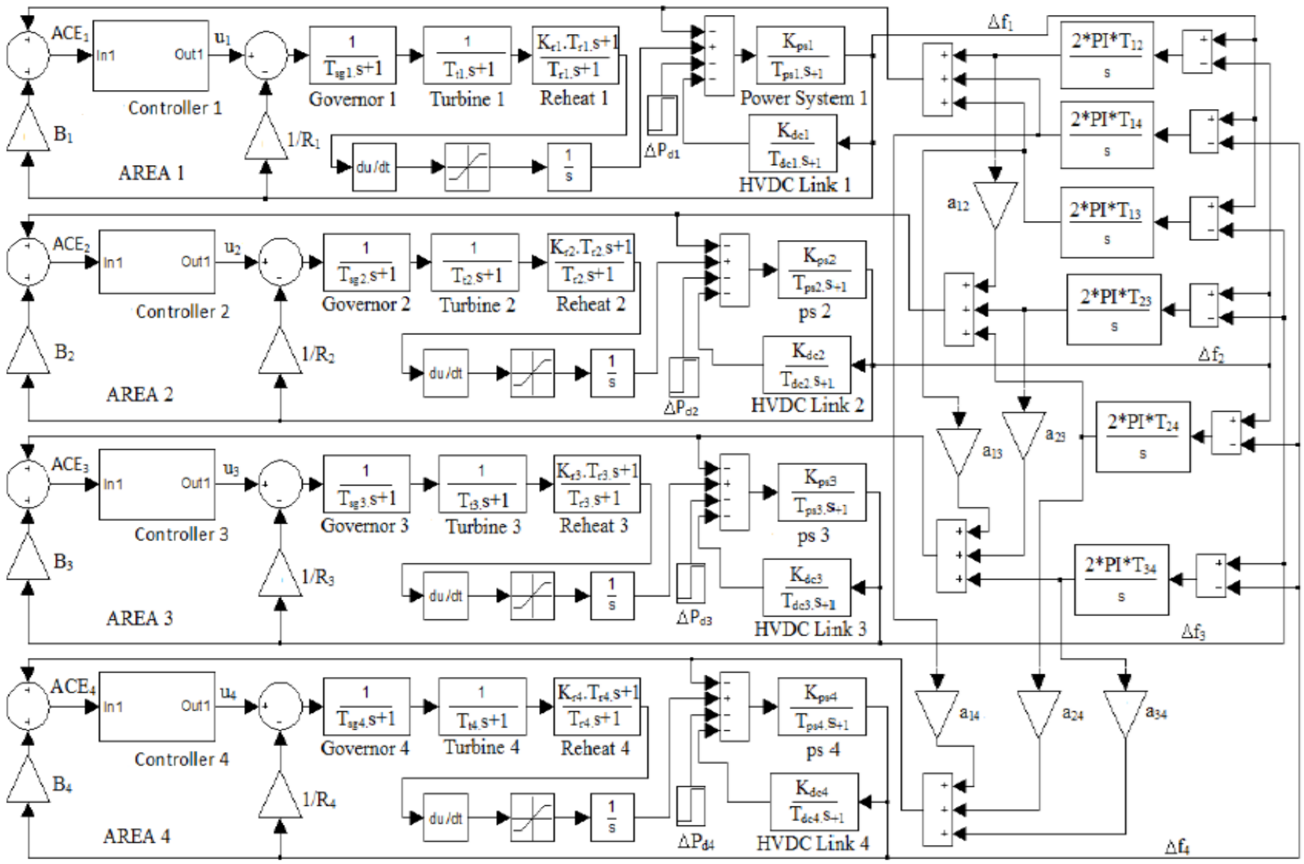

Fig. 2 Simulation model (built on MATLAB/Simulink) of a 4-area interconnected electric power grid under the current study

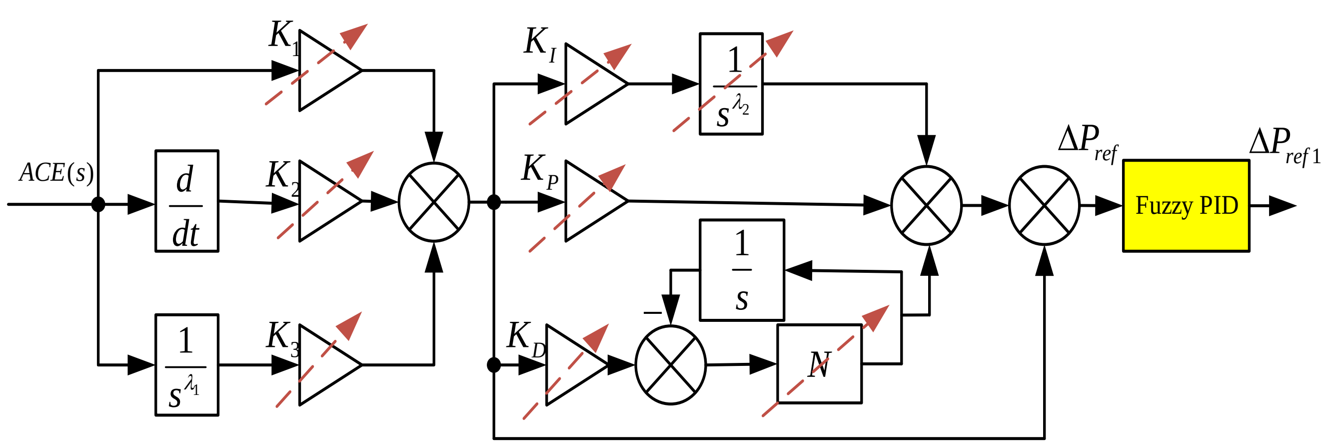

Fig. 3 The integrated model of the proposed load-frequency controller

Input: *N, D, Maxiter*
Output: *The final optimized result*
Begin
Initializing (Randomly generate the initial positions for N wolves within the defined search space, then evaluate the fitness of each wolf).
For *iter = 2 to Maxiter*
Find Xα, Xβ, and Xδ.
For *i = 1 to N*
Calculate the components X_{i1}, X_{i2}, and X_{i3} for the current wolf X_i, $X_{i1}(t) = X_{\alpha}(t) - A_{i1}(t).D_{\alpha}(t)$ $X_{i2}(t) = X_{\beta}(t) - A_{i2}(t).D_{\beta}(t)$, $X_{i3}(t) = X_{\delta}(t) - A_{i3}(t).D_{\delta}(t)$
Compute the average guided position $X_{i\_GWO}(t+1)$ for the current iteration $X(t+1) = \dfrac{X_{i1}(t) + X_{i2}(t) + X_{i3}(t)}{3}$
Determine the radius $R_i(t)$ for the local search space of wolf X_i at iteration t based on $R_i(t) = \left\| X_i(t) - X_{i-GWO}(t+1) \right\|$
Establish the neighborhood for wolf X_i with the calculated radius $R_i(t)$
For *d = 1 to D*
$X_{i-DLH,d}(t+1) = X_{i,d}(t) + rand \times (X_{n,d}(t) - X_{r,d}(t))$
End for
Selecting best ($X_{i-GWO}(t+1)$, $X_{i-DLH}(t+1)$).
Update Population.
End for
End for
Return the best-found solution.
End

Fig. 4 Pseudo-code illustrating the *i*GWO algorithm as applied in this investigation

Table 1. Fuzzy logic rules for Kp, Ki, and Kd

		ΔPref1						
		VLN	MN	SLN	NEU	SLP	MP	VLP
dΔPref1	VLN	VLP	VLP	VLP	MP	SLP	NEU	NEU
	MN	VLP	VLP	MP	SLP	NEU	NEU	SLN
	SLN	VLP	VLP	MP	SLP	NEU	SLN	MN
	NEU	MP	MP	NEU	SLN	SLN	MN	MN
	SLP	MP	MP	SLP	NEU	SLN	MN	VLN
	MP	SLP	SLP	NEU	SLN	MN	MN	VLN
	VLP	NEU	NEU	SLP	SLN	MN	VLN	VLN

VLN: Very Large Negative, MN: Medium Negative, SLN: Small Negative, NEU: Neutral, SLP: Small Positive, MP: Medium Positive, VLP: Very Large Positive

Key improvements to the algorithm involve incorporating a refined search strategy, which is seamlessly integrated via a dedicated selection and update phase. This specific architectural enhancement is highlighted by a dashed border in the iGWO diagram, presented in Figure 4. Structurally, the iGWO algorithm comprises three primary stages: initialization, a movement and exploration phase, and a concluding selection and update operation. The entire pseudo code of the iGWO is graphically detailed in Figure 4

The method for optimizing *i*GWO control parameters $K_1, K_2, K_3, \lambda_1, K_P, K_I, K_D, \lambda_1, N$ is based on an objective function. The objective function defined for this controller is presented in Equation 1. In this equation, Δf_i (i = 1, 2, 3, 4) are the frequency deviations in the respective areas, and ΔP_{tie} represents the power change on the tie-line between areas. Here, τ_s denotes the simulation time, which is considered in Section 4 of this paper. Criterion (1) is also considered the IATE (Integral Absolute Time Error), which should be an effective index to evaluate the performance of a control system.

$$J = IATE = \int_0^{\tau_s} \left(|\Delta f_1| + |\Delta f_2| + |\Delta f_3| + |\Delta f_4| + \sum_{i,k=1}^{4} |\Delta P_{tie\,i,k}| \right) t\, dt \qquad (1)$$

To further improve the system's stability, the study utilizes a fuzzy PID controller with two inputs ΔP_{ref1}, $d\Delta P_{ref1}$

and three outputs, Ki, Kp, and Kd, which have 7 standard triangle-type membership functions and a typical fuzzy rule base as presented in Table 1.

4. Numerical Simulation Results and Discussions

To undertake a **rigorous and comprehensive** evaluation of the precisely engineered control strategy's efficacy, this seminal study embarks upon an in-depth simulation of the intricately interconnected multi-area power system. This sophisticated modeling approach is meticulously designed to mirror real-world operational complexities by integrating a diverse array of Renewable Energy Sources (RESs), which inherently introduce fluctuations and uncertainties into the grid dynamics. Furthermore, the simulation explicitly accounts for the presence and influence of High-Voltage Direct Current (HVDC) transmission links, which are crucial elements in modern long-distance power transfer and grid stability. Beyond these critical infrastructure components, the assessment also incorporates a wide spectrum of varying load disturbances, meticulously chosen to represent realistic demand patterns across different times and conditions, each characterized by its unique shape and amplitude. This multifaceted analysis is systematically conducted across three distinct and challenging scenarios, each specifically crafted to expose the controller's resilience, adaptability, and superior performance under a range of operational stresses, thereby providing a robust foundation for validating its practical applicability and effectiveness in contemporary power grid environments.

4.1. Scenario 1

All loads are treated as steps with the magnitudes for all four load changes of 5%.

Simulation results are provided in Figure 5 (a), (b), (c), and (d) for all control areas concerning three controllers: the traditional PID regulator, the GWO-PID one, and the proposed hybrid controller. The dynamic responses are network frequency deviations from the nominal value of 50 Hz in Vietnam.

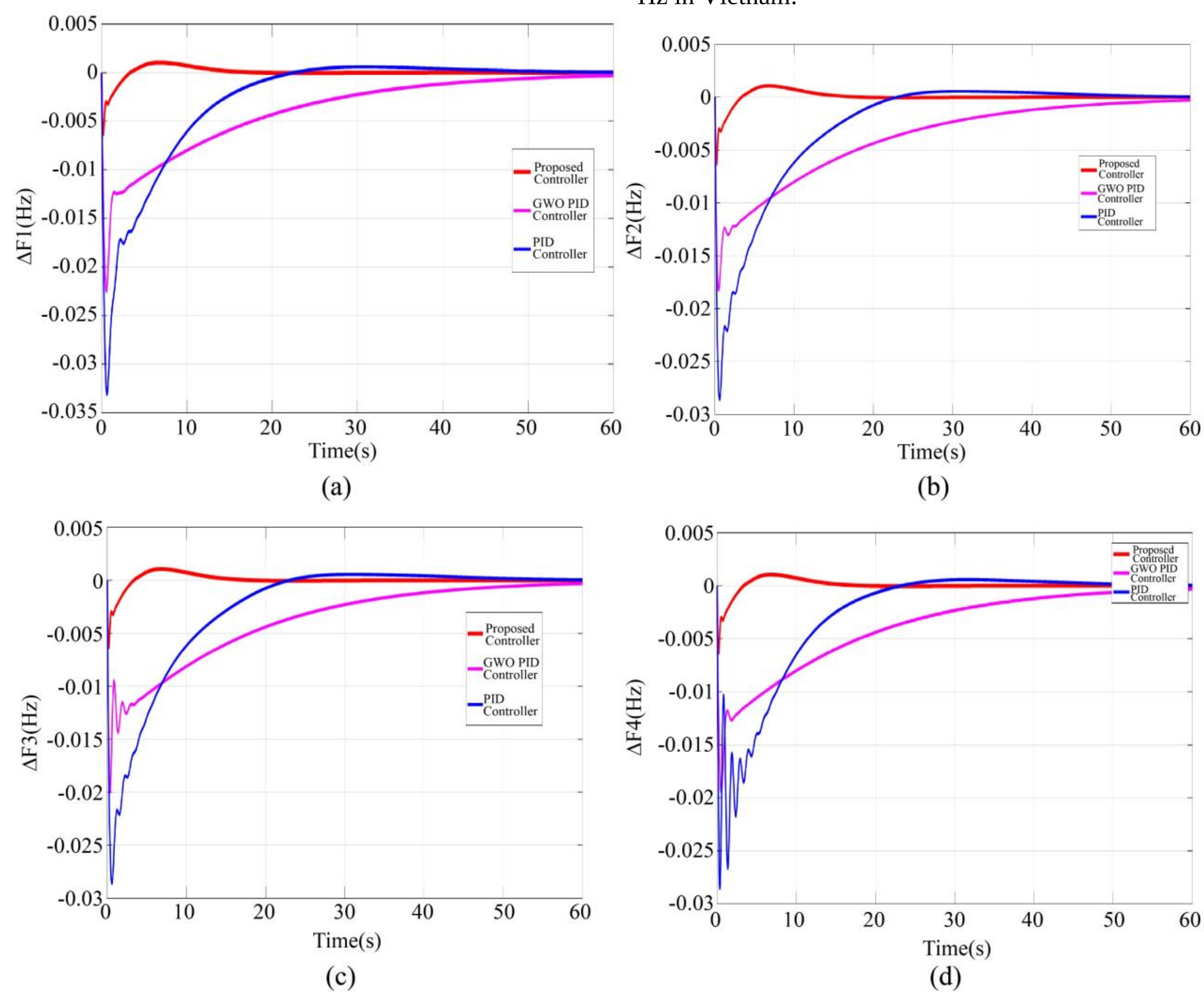

Fig. 5 Frequency Deviation Dynamics across Four Areas (Scenario 1). (a) Area 1 (ΔF1), (b) Area 2 (ΔF2), (c) Area 3 (ΔF3), (d) Area 4 (ΔF4).

4.2. Scenario 2

In this scenario, pulse-type load disturbances are concurrently applied to all four control areas of the power system. The resulting simulation outcomes, illustrating the system's dynamic behavior, are presented in Figure 6 (a), (b), (c), and (d).

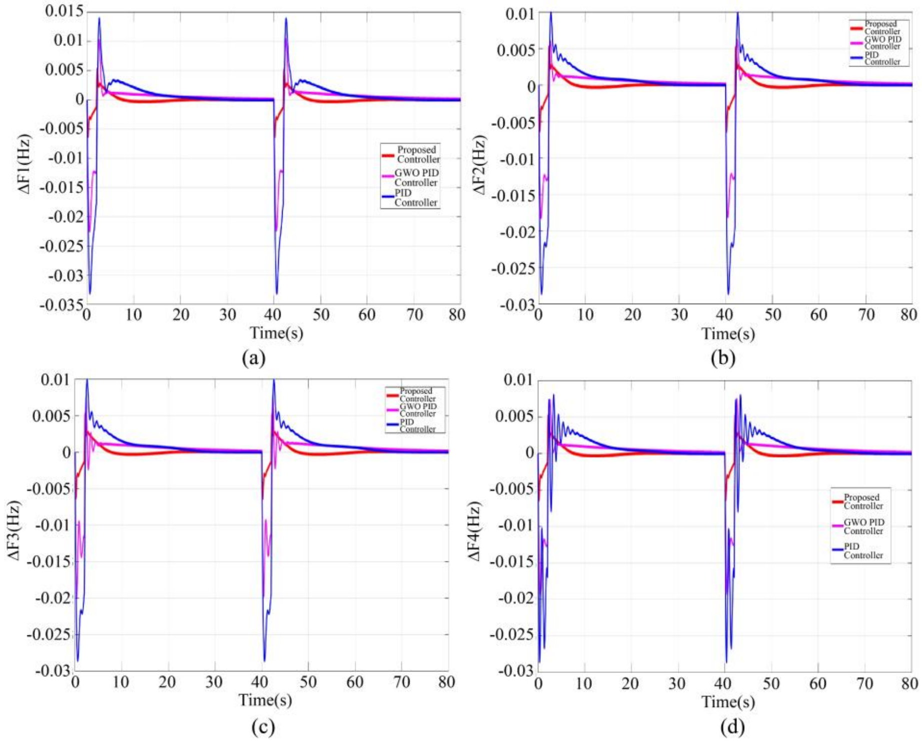

Fig. 6 Frequency Deviation Dynamics across Four Areas (Scenario 2). (a) Area 1 (ΔF1), (b) Area 2 (ΔF2), (c) Area 3 (ΔF3), (d) Area 4 (ΔF4)

4.3. Scenario 3

Loads randomly change in all four control areas. In this context, Figure 7 presents simulation results executed in MATLAB/Simulink.

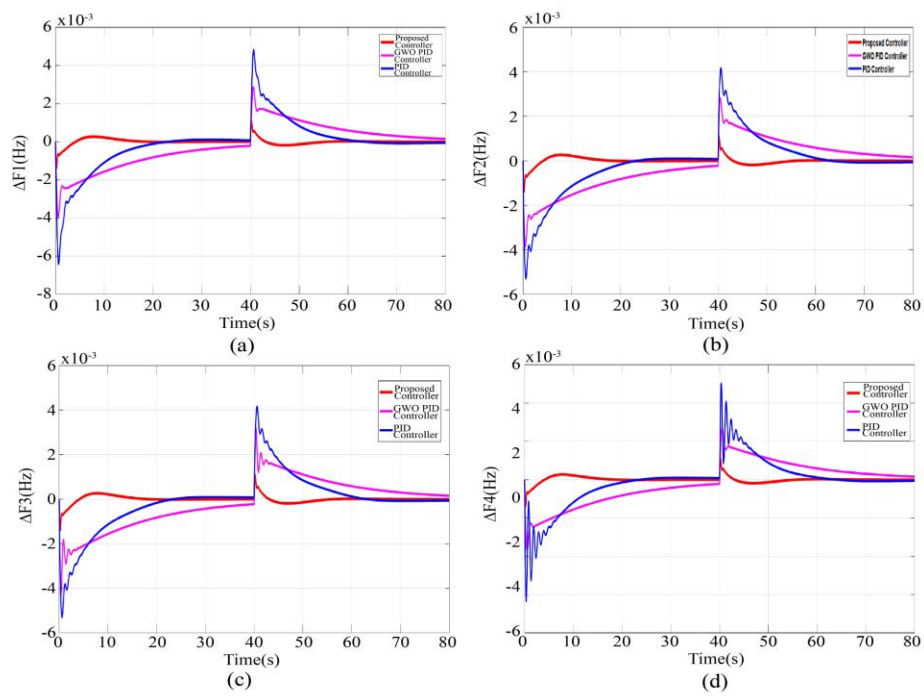

Fig. 7 Frequency Deviation Dynamics across Four Areas (Scenario 3) (a) Area 1 (ΔF1), (b) Area 2 (ΔF2), (c) Area 3 (ΔF3), (d) Area 4 (ΔF4)

As vividly illustrated in Figures 5, 6, and 7, the frequency error responses across each of the four interconnected areas unequivocally demonstrate the superior performance of our proposed multi-layered control strategy. A meticulous analysis of these comparative results reveals that the designed controller consistently achieves significantly enhanced control performances, characterized by minimal frequency errors and notably reduced settling times. In stark contrast, the traditional PID controller consistently exhibits the most pronounced deviations and considerably prolonged settling times, thereby unequivocally substantiating the unparalleled dynamic performance of our hybrid intelligent controllers when benchmarked against conventional PID approaches.

The inherent complexity of modern interconnected power systems, exacerbated by their high dimensionality and the parametric variability encountered during operational transients, presents a formidable control challenge. Furthermore, while crucial for sustainable energy, the pervasive integration of Renewable Energy Sources (RESs) paradoxically exacerbates frequency stabilization difficulties across these interconnected areas by introducing significant intermittency and reducing system inertia. As powerfully evidenced by the simulation outcomes presented in Figures 5, 6, and 7, controllers relying on simplistic methodologies or less sophisticated optimization techniques consistently exhibit degraded performance under these demanding conditions.

The efficacy of our Fuzzy-PID controller architecture, as detailed in Figure 3, plays a pivotal role. Through the judicious selection of fuzzy sets, the precise generation of input membership functions, and the robust application of rule-based inference, the Fuzzy-PID controller demonstrably achieves a superior control quality when directly compared to both conventional PID and existing GWO-PID controllers.

Crucially, the seamless integration of the innovative iGWO algorithm for optimizing the parameters of our cascaded PID and Fuzzy-PID controllers is the cornerstone of this enhanced stability. This advanced optimization methodology enables the control system to effectively maintain frequency stability within stringent acceptable operational limits, even amidst the profound system complexities that arise from the substantial penetration of renewable energy sources and the dynamic operation of HVDC transmission links. The results consistently highlight the proposed method's ability to achieve faster rise times, negligible overshoot, and rapid settling times, definitively establishing its optimal control capability over its counterparts.

5. Conclusion and Future Work

It should be found that the maintenance of network frequency stability within power systems constitutes a critical and pressing challenge in contemporary power system operation and distribution. However, the presence of inherent nonlinearities, The escalating proliferation of HVDC transmission links, coupled with the pervasive and increasing integration of renewable energy sources introduces substantial complexities into contemporary power systems. These factors collectively intensify the formidable challenge of achieving robust and reliable frequency stabilization, a critical prerequisite for grid operational integrity. Consequently, this study undertakes a series of comprehensive comparative simulation analyses designed to rigorously ascertain and evaluate the efficacy of diverse control methodologies under these demanding conditions. They have obviously demonstrated that hybrid intelligent controllers, an integration of $PI^{\lambda 1}D$ - $PI^{\lambda 2}DF$ and Fuzzy-PID controllers applying the *i*GWO mechanism, consistently outperform traditional control schemes in terms of dynamic performance and frequency regulation. The novel research trajectory pursued in this study involves investigating and developing a high-performance control strategy tailored for interconnected power systems characterized by multiple generating units within each control area. Furthermore, future research endeavors will focus on exploring the practical implementation and deployment of the hybrid load frequency controllers investigated herein, with a particular emphasis on addressing real-world operational constraints and enhancing system resilience.

References

[1] Mohamed A. Mohamed et al., "A Novel Adaptive Model Predictive Controller for Load Frequency Control of Power Systems Integrated with DFIG Wind Turbines," *Neural Computing and Applications*, vol. 32, no. 11, pp. 7171-7181, 2019. [CrossRef] [Google Scholar] [Publisher Link]

[2] Israfil Hussain et al., "Performance Analysis of Flower Pollination Algorithm Optimized PID Controller for Wind-PV-SMES-BESS-Diesel Autonomous Hybrid Power System," *International Journal of Renewable Energy Research*, vol. 7, no. 2, pp. 643-651, 2017. [CrossRef] [Google Scholar] [Publisher Link]

[3] Thongchart Kerdphol, Fathin Saifur Rahman, and Yasunori Mitani, "Virtual Inertia Control Application to Enhance Frequency Stability of Interconnected Power Systems with High Renewable Energy Penetration," *Energies*, vol. 11, no. 4, pp. 1-16, 2018. [CrossRef] [Google Scholar] [Publisher Link]

[4] Meysam Gheisarnejad, "An Effective Hybrid Harmony Search and Cuckoo Optimization Algorithm Based Fuzzy PID Controller for Load Frequency Control," *Applied Soft Computing*, vol. 65, pp. 121-138, 2018. [CrossRef] [Google Scholar] [Publisher Link]

[5] E.S. Ali, and S.M. Abd-Elazim, "BFOA Based Design of PID Controller for Two Area Load Frequency Control with Nonlinearities," *International Journal of Electrical Power and Energy Systems*, vol. 51, pp. 224-231, 2013. [CrossRef] [Google Scholar] [Publisher Link]

[6] Sukhwinder Singh Dhillon, J.S. Lather, and S. Marwaha, "Multi Objective Load Frequency Control Using Hybrid Bacterial Foraging and Particle Swarm Optimized PI Controller," *International Journal of Electrical Power and Energy Systems*, vol. 79, pp. 196-209, 2016. [CrossRef] [Google Scholar] [Publisher Link]

[7] Dianwei Qian et al., "Load Frequency Control by Neural-Network-Based Integral Sliding Mode for Nonlinear Power Systems with Wind Turbines," *Neurocomputing*, vol. 173, pp. 875-885, 2016. [CrossRef] [Google Scholar] [Publisher Link]

[8] Andreas Ulbig et al., "Predictive Control for Real-Time Frequency Regulation and Rotational Inertia Provision in Power Systems," *52nd IEEE Conference on Decision and Control*, Firenze, Italy, pp. 2946-2953, 2013. [CrossRef] [Google Scholar] [Publisher Link]

[9] Mohamed Mostafa Elsaied et al., "Application of Different Optimization Techniques to Load Frequency Control with WECS in a Multi-Area System," *Electric Power Components and Systems*, vol. 46, no. 7, pp. 739-756, 2018. [CrossRef] [Google Scholar] [Publisher Link]

[10] Dipayan Guha, Provas Kumar Roy, and Subrata Banerjee, "Application of Backtracking Search Algorithm in Load Frequency Control of Multi-Area Interconnected Power System," *Ain Shams Engineering Journal*, vol. 9, no. 2, pp. 257-276, 2018. [CrossRef] [Google Scholar] [Publisher Link]

[11] Prasun Sanki, and Mousumi Basu, "New Approach in Two-Area Interconnected AGC Including Various Renewable Energy Sources Using PSO," *Turkish Journal of Electrical Engineering and Computer Sciences*, vol. 26, no. 3, pp. 1491-1504, 2018. [CrossRef] [Google Scholar] [Publisher Link]

[12] Partha Pratim Dey et al., "Active Power Management of Virtual Power Plant under Penetration of Central Receiver Solar Thermal-Wind Using Butterfly Optimization Technique," *Sustainability*, vol. 12, no. 17, pp. 1-16, 2020. [CrossRef] [Google Scholar] [Publisher Link]

[13] Farag K. Abo-Elyousr, and Almoataz Y. Abdelaziz, "A Novel Modified Robust Load Frequency Control for Mass-Less Inertia Photovoltaics Penetrations via Hybrid PSO-WOA Approach," *Electric Power Components and Systems*, vol. 47, no. 19-20, pp. 1744-1758, 2019. [CrossRef] [Google Scholar] [Publisher Link]

[14] Zaheeruddin, and Kavita Singh, "Primary Frequency Regulation of a Microgrid by Deloaded Tidal Turbines," *Soft Computing*, vol. 24, no. 19, pp. 14667-14685, 2020. [CrossRef] [Google Scholar] [Publisher Link]

[15] Alhassan H. Alattar et al., "Performance Enhancement of Micro Grid System with SMES Storage System Based on Mine Blast Optimization Algorithm," *Energies*, vol. 12, no. 16, pp. 1-23, 2019. [CrossRef] [Google Scholar] [Publisher Link]

[16] Sudhanshu Ranjan et al., "Parabolic Trough Solar-Thermal-Wind-Diesel Isolated Hybrid Power System: Active Power/Frequency Control Analysis," *IET Renewable Power Generation*, vol. 12, no. 16, pp. 1893-1903, 2018. [CrossRef] [Google Scholar] [Publisher Link]

[17] Jinsong Liu et al., "Integrated System Design for a Large Wind Turbine Supported on a Moored Semi-Submersible Platform," *Journal of Marine Science and Engineering*, vol. 6, no. 1, pp. 1-25, 2018. [CrossRef] [Google Scholar] [Publisher Link]

[18] Taufik Roni Sahroni, "Modeling and Simulation of Offshore Wind Power Platform for 5 MW Baseline NREL Turbine," *The Scientific World Journal*, vol. 2015, no. 1, pp. 1-11, 2015. [CrossRef] [Google Scholar] [Publisher Link]

[19] J. Jonkman et al., "*Definition of a 5-MW Reference Wind Turbine for Offshore System Development*," OSTI OAI (U.S. Department of Energy Office of Scientific and Technical Information), 2009. [CrossRef] [Google Scholar] [Publisher Link]

[20] Irfan Ahmed Khan et al., "Load Frequency Control in Power Systems with High Renewable Energy Penetration: A Strategy Employing PI^λ (1+PDF) Storage, and IPFC-FACTS," *Alexandria Engineering Journal*, vol. 106, pp. 337-366, 2024. [CrossRef] [Google Scholar] [Publisher Link]

Appendix

The simulation of the four-area power system was conducted using the following defined parameters:

- **Nominal Power Rating (Pr):**
  - Area 1: Pr1=2000 MW
  - Area 2: Pr2=4000 MW
  - Area 3: Pr3=8000 MW
  - Area 4: Pr4=10000 MW
- **Speed Regulation (R):** For all areas, R1=R2=R3=R4=2.4 Hz/p.u.MW
- **Frequency Bias Coefficient (B):** Consistent across all areas, B1=B2=B3=B4=0.425 Hz/p.u.MW
- **System Time Constants:**
  - Governor Time Constant (Tsg): Tsg1=Tsg2=Tsg3=Tsg4=0.08 s
  - Turbine Time Constant (Tt): Tt1=Tt2=Tt3=Tt4=0.3 s
  - Power System Time Constant (Tps): Tps1=Tps2=Tps3=Tps4=20 s
- **Power System Gain (Kps):** Kps1=Kps2=Kps3=Kps4=120 HZ/p.u.MW
- **Tie-Line Synchronizing Coefficients (Tij):** For inter-area connections, T12=T13=T14=T23=T24=T34=0.086

p.u.MW/Radin

- **Area Participation Factors (aij):** Calculated as the ratio of nominal power, aij=−Pri/Prj
- **Reheat Time Constant (Tr):** For reheat turbines, Tr1=Tr2=Tr3=Tr4=10 s
- **Reheat Coefficient (Kr):** Kr1=Kr2=Kr3=Kr4=0.5
- **Maximum Tie-Line Power (Ptie,max):** Ptie,max=200 MW
- **Nominal System Frequency (f):** f=50 Hz (typical for Vietnam)
- **HVDC Gain Constant (Kdc):** Kdc1=Kdc2=Kdc3=Kdc4=1.0
- **HVDC Time Constant (Tdc):** Tdc1=Tdc2=Tdc3=Tdc4=0.2 s.